Journal of Molecular Liquids 313 (2020) 113491

Contents lists available at ScienceDirect

Journal of Molecular Liquids

journal homepage: www.elsevier.com/locate/molliq

FTIR spectroscopic studies and DFT calculations on the binary solution of methyl acetate with m-xylene

N.K. Karthick [a], G. Arivazhagan [b,*], P.P. Kannan [c]

[a] Department of Physics, The Madura College, Madurai 625011, Tamil Nadu, India
[b] Department of Physics, Thiagarajar College, Madurai 625009, Tamil Nadu, India
[c] Postgraduate Department of Physics, Mannar Thirumalai Naicker College, Madurai 625004, Tamil Nadu, India

ARTICLE INFO

Article history:
Received 3 April 2020
Received in revised form 25 May 2020
Accepted 30 May 2020
Available online 01 June 2020

Keywords:
Hydrogen bond
Homointeraction
Heterointeraction
Dimer
Stability
Complex

ABSTRACT

FTIR spectra have been recorded for pure methyl acetate, pure m-xylene and their equimolar binary solution. Shifts have been observed in all the vibrational modes of methyl acetate, m-xylene in the solution indicating the possibilities for molecular interactions. To get more precise information on the molecular interactions, DFT calculations have been performed. From these calculations it is found that methyl acetate dimers of four different geometries are possible. The most stable among these dimers is the one with $C-H\cdots O=C$ interactions stronger than the $C-H\cdots O-C$. If the scenario is opposite in a dimer, the stability becomes the least. These four dimers dissociate in the investigated binary solution and 1:2 (m-xylene:methyl acetate) complexes of five different geometries are formed. In one of the complexes, the homointeractions $C-H\cdots O=C$ among the methyl acetate molecules are more stronger than any other interactions and the stability of the complex is the least. In all the other complexes the interactions $(methyl\ acetate)C-H\cdots\pi\ (m-xylene)$ are the strongest. In complexes where the hydrogens attached to ring carbons of m-xylene do not involve in hydrogen bonds with methyl acetate, the stability of the complexes is more. If these hydrogen bonds are formed, the stabilities of those complexes are reduced.

1. Introduction

Since 1960s, large amount of data on organic systems containing carbonyl group is available [1] in which hydrogen bond (H-bond) interactions between these systems and various polar, non-polar solvents were investigated. These interactions in the above mentioned systems were investigated mainly because of their importance in fields of physical chemistry, crystal and supramolecular engineering, biochemistry [2–4]. For instance, the carbonyl group $C=O$ can serve as a good candidate to probe the local electric field fluctuations due to H-bond interactions in protein interfaces. Because the frequency corresponding to the stretching mode of carbonyl group has a linear dependence on the electric field due to these H-bond interactions in proteins [5]. In particular the carbonyl group in an ester is preferred due to the fact that there is no overlapping of the protein vibrational modes onto the carbonyl stretching modes in the IR region at a neutral pH value [6]. In the category of esters, methyl acetate is the second simplest methyl ester after methyl formate and a viable alternative for a number of more hazardous solvents because of its low toxicity, as stated by Sunahori et al. [7]. Such an industrially important ester, methyl acetate had been subjected to investigation by many scientists [4,8–11] whose focus was mainly on the ability of this ester to form heteromolecular H-bonds with other solvents. But methyl acetate possesses two methyl groups, a carbonyl oxygen and an alkoxy oxygen which opens up the possibilities for the ester to involve in self-association through H-bonds. So far people have not made an attempt to investigate these possibilities which prompted us to take up this research problem in the present work. We have employed Fourier Transform Infrared (FTIR) Spectroscopy and Density Functional Theory (DFT) calculations in the present investigation to see if methyl acetate molecules can self-associate among themselves. If this is possible, then it is also very interesting to find out whether the carbonyl oxygen or the alkoxy oxygen of methyl acetate involves in self-association. Such kind of investigations on site specific interactions among the self-associated molecular networks of formamide had already been carried out by Frey and Leutwyler [12], Vargas et al. [13]. These investigators [12,13] had studied the self-association among formamide molecules and found that self-association results in formamide dimers of five different geometries. These scientists reported that either or both of the interactions $N-H\cdots O=C$ and $C-H\cdots O=C$ are possible in these dimers which confirms that more than one type of homointeraction may be responsible for self association. In the present work too, there are chances for two types of homointeractions

* Corresponding author at: Thiagarajar College, Madurai 625009, Tamil Nadu, India.
E-mail addresses: arivuganesh@gmail.com, arivazhagan_physics@tcarts.in (G. Arivazhagan).

https://doi.org/10.1016/j.molliq.2020.113491
0167-7322/

$C-H\cdots O=C$ and $C-H\cdots O-C$ among the methyl acetate molecules which can lead to self association. These chances have been investigated in the present work by combining Natural Bonding Orbital (NBO) analyses and second order perturbation energy E(2) profiles along with FTIR spectral studies, theoretical frequency calculations. The purpose of incorporating E(2) profile is to predict the strengths of various interactions in self-associated methyl acetate networks, if any of these are possible. The stabilities of these possible self-associated species have also been ascertained from their interaction energies, obtained through DFT calculations. The question of whether these self-associated methyl acetate networks can preserve their self-association in the environment of non-polar solvent m-xylene is another objective of the present work. This binary solution methyl acetate + m-xylene has been chosen in the present work since Sastry et al. [14] had found excess molar volumes, viscosity deviations, excess isentropic compressibilities and deviations in relative permittivities of the solution. In this work they did not discuss anything about the presence or absence of H-bonds (both homomolecular and heteromolecular) in this solution. Therefore, in the present work we have investigated the chances for these H-bonds in this binary solution using FTIR spectral studies and DFT calculations. These kind of bonds in a binary system leads to the formation of molecular complexes of different stoichiometries [15,16] and the strengths of molecular interactions in these complexes can be compared from the E (2) profiles. Therefore, in the present work we have studied the possibilities of molecular complexation too in the binary solution of methyl acetate with m-xylene. There are no previous reports in literature for similar kind of studies on this binary solution.

2. Materials and methods

Methyl acetate (MA) - anhydrous - 99.5% was procured from Sigma Aldrich, USA. m-Xylene (MXY)- Pure Assay (GC 98%) was purchased from Sisco Research Laboratories (SRL) Pvt. Ltd., Mumbai, India. Both these chemicals were used as such without any purification. FTIR spectra for pure MA, MXY and their equimolar binary solution (MAMXY) were recorded with a resolution of 1 cm^{-1} at room temperature using a Perkin Elmer FTIR spectrophotometer (model: Spectrum RXI).

Geometry optimization, frequency calculation and NBO analyses in the present work were done using a Gaussian 09W programme package [17]. The method used for the above mentioned DFT calculations was B3LYP-D3 which is a combination of the functional B3LYP [18] and D3 level of Grimme's dispersion correction [19]. 6-311++G (d,p) basis set was used.

3. Results and discussion

3.1. FTIR spectroscopic studies

In the FTIR spectrum of pure MA (Fig. 1a, Table 1) the peaks at 2964 and 2854 cm^{-1} are assigned to $\nu_{as}(CH_3)$ and $\nu_s(CH_3)$, respectively. Both the $C=O$ stretching bands of pure MA and the binary solution have been deconvoluted into two Gaussian peaks (Fig. 1d and e). $C=O$ stretching in pure MA contributes to two peaks at 1780 and 1761 cm^{-1} (Fig. 1a, Table 1). The former is mentioned as ν_{higher} $(C=O)$ and the latter as ν_{lower} $(C=O)$ in this research article just for an ease in representation. Such kind of more than one peak for the $C=O$ stretching mode of MA has been reported previously, not for this ester in its pure form but for it in the environment of other solvents [4,8–11]. For instance, two peaks for this mode had been observed in the environment of heavy water [10] and it is believed that the peak at higher wavenumber is due to the carbonyl oxygen of MA singly H-bonded to water. One more H-bond with water results in another peak at lower wavenumber. The intensities of the peaks had been compared by Fang et al. [11] and they found that the peak at higher wavenumber has lower intensity. But this result was in contradiction to the populations of these singly and doubly H-bonded species obtained through molecular dynamics simulations, which were found to be 51% and 44%, respectively [11]. The investigators [11] have mentioned in their work that this discrepancy may be due to the fact that they did not consider the effect of H-bond on the alkoxy oxygen of MA. Then they improved their calculations by taking this H-bond into account and decomposed the carbonyl stretching mode in MA- water solutions into contributions from different H-bonded configurations. The investigators have mentioned the following five types of configurations in their work: 1) two H-bonds on the carbonyl oxygen (dc) and no H-bond on the alkoxy oxygen (na) of MA, 2) two H-bonds on the carbonyl oxygen and one H-bond on the alkoxy oxygen (sa) of MA, 3) one H-bond on the carbonyl oxygen (sc) and no H-bond on the alkoxy oxygen of MA, 4) one H-bond each on the carbonyl oxygen and alkoxy oxygen of MA, 5) no H-bond on the carbonyl oxygen (nc) and one H-bond on the alkoxy oxygen of MA. From this analysis they have concluded that both dc/sa and sc/na with a total population of 40.0% contribute to the $C=O$ stretching peak at lower wavenumber. On the other hand, the peak at higher wavenumber is a consequence of the sc/sa moieties with a total population of 28.1%. These recalculated populations explain the difference in intensities of the two peaks observed earlier by Fang et al. [11] and firmly establishes the notion that H-bond on the alkoxy oxygen of MA in MA-water solutions has a significant role to play on the $C=O$ stretching mode of MA. This result may be used to explain the two $C=O$ stretching bands for pure MA in the present work wherein H-bonds may be formed both on the alkoxy oxygen and carbonyl oxygen of MA. But here these H-bonds are due to the self-association of MA unlike as in the case of MA- water solutions where the H-bonds are of heteromolecular in nature [10]. Heteromolecular H-bonds in ethyl acetate – nitrobenzene binary solution playing a role in producing a doublet in the $C=O$ stretching region of ethyl acetate, have been reported by our research group recently [20]. In that work we found that formation of ethyl acetate dimers with closed geometry is possible via the H-bonds that involve only the alkoxy oxygen and not the carbonyl oxygen. This led us to conclude that these dimers are the causative factor behind the single carbonyl stretching peak in the FTIR spectrum of pure ethyl acetate [20]. Dissociation of these dimers and formation of ethyl acetate – nitrobenzene complexes consisting of (*nitrobenzene*) $C-H\cdots O$ (*ethyl acetate*) contacts in the ethyl acetate – nitrobenzene binary solution was confirmed through DFT calculations in that work. These contacts include both the carbonyl and alkoxy oxygens of ethyl acetate. This result supports the appearance of two $C=O$ stretching peaks in the binary solution for ethyl acetate [20] which is also an ester as like MA. These inferences strengthen the speculations on self-association of MA which may possess H-bonds on both the alkoxy oxygen and carbonyl oxygen explaining a doublet for $C=O$ stretching in its FTIR spectrum (Fig. 1a, Table 1). The band at 1248 cm^{-1} in this spectrum is assigned to the $\nu\,(C-C-O)$ of MA.

The peak at 2927 cm^{-1} in the FTIR spectrum of pure MXY (Fig. 1b, Table 1) is due to $\nu_{as}(CH_3)$. The ring deformation vibrations of this molecule produce a peak at 1169 cm^{-1}. The symmetric and asymmetric stretching vibrations of the other $C-H$ present in the aromatic ring of MXY produce peaks at 3058 cm^{-1} and 3019 cm^{-1}, respectively. The conventions “symmetric” and “asymmetric” described for the $C-H$ stretching modes of MXY (except $\nu_{as}(CH_3)$) in the present work are used to differentiate the modes in which all the $C-H$ undergo in-phase (symmetric) stretching and out of phase (asymmetric) stretching. Such kind of conventions for the $C-H$ stretching modes have earlier been used by Kraanie et al. [21] for toluene which has single substitution on its ring. Our research group too has reported similar results for toluene in our recent works [22,23]. From these results [21–23] it may be opined that substitution on an aromatic ring is the main reason behind the $\nu_s(C-H)$ and $\nu_{as}(C-H)$ peaks in FTIR spectrum, which is also found to be applicable in the present work for MXY which has two substitutions on its ring. Blue shifts in both these peaks and also a red shift in $\nu_{as}(CH_3)$ of MXY in the FTIR spectrum of the binary solution MAMXY (Fig. 1c, Table 1) may be due to the interactions (*MXY*

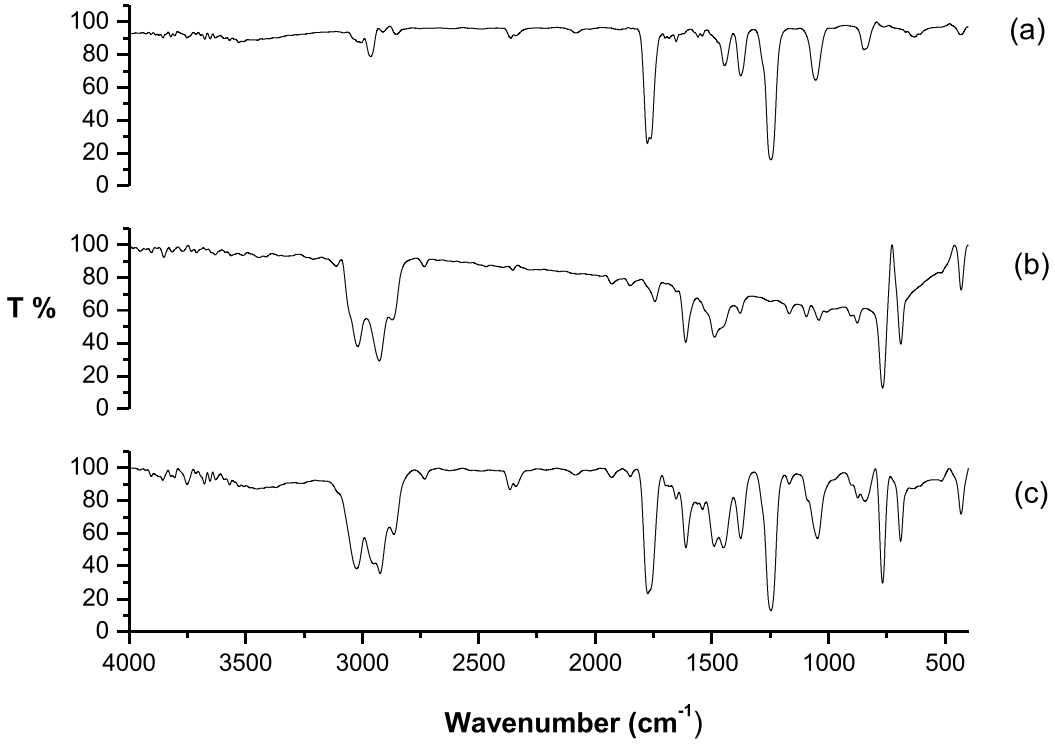

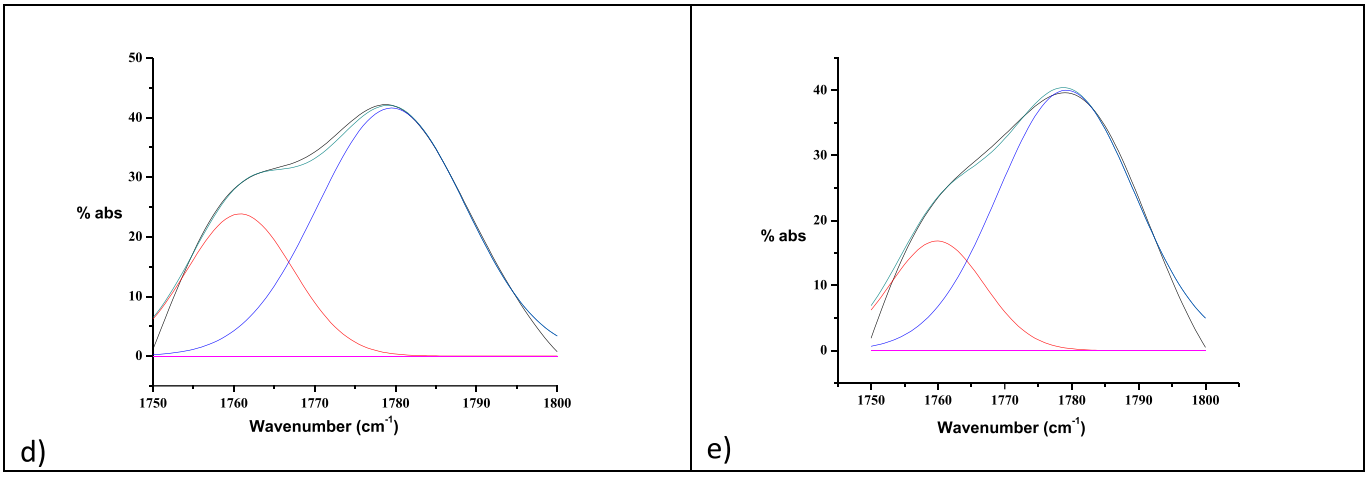

Fig. 1. FTIR spectrum of (a) pure methyl acetate (MA) (b) pure m-xylene (MXY) (c) equimolar binary solution of methyl acetate with m-xylene (MAMXY). Deconvoluted Gaussian peaks of the $C = O$ stretching band of (d) MA (1761 and 1780 cm^{-1}) and (e) MAMXY (1760 and 1779 cm^{-1}).

Table 1
Experimental FTIR spectral band assignments for pure methyl acetate (MA), m-xylene (MXY) and their equimolar binary solution (MAMXY).

Vibrational mode	Wavenumber (cm^{-1})		
	Pure MA	Pure MXY	MAMXY solution
$\nu_{as}(CH_3)$	2964		2951
$\nu_s(CH_3)$	2854		2864
$\nu_{higher}\ (C = O)$[a]	1780		1779
$\nu_{lower}\ (C = O)$[b]	1761		1760
$\nu\ (C - C - O)$	1248		1248
$\nu_s(C - H)$		3058	3105
$\nu_{as}(C - H)$		3019	3024
$\nu_{as}(CH_3)$		2927	2923
Ring deformation		1169	1169

ν - stretching; *as* - asymmetric; *s* - symmetric.
[a] $C = O$ stretching peak at higher wavenumber.
[b] $C = O$ stretching peak at lower wavenumber.

ring/methyl) $C - H\cdots O$ (*carbonyl oxygen of MA*). The possibilities for these interactions are well supported by the red shifts (Fig. 1a, Table 1) in $\nu_{higher}\ (C = O)$ and $\nu_{lower}\ (C = O)$ modes of MA in the solution. In this solution the shifts in $\nu_{as}(CH_3)$ and $\nu_s(CH_3)$ modes of MA may be due to the dissociation of MA and/or the heterointeractions (*MA*) $C - H\cdots\pi$ (*MXY*). The shifts in MA CH_3 stretching modes in the solution may happen even in case of the absence of heterointeractions (*MA*) $C - H\cdots\pi$ (*MXY*) and dissociation of MA. This is because the methyl group present in MA may be affected by the heterointeractions (*MXY ring/methyl*) $C - H\cdots O$ (*carbonyl oxygen of MA*) happening in its vicinity. This belief is due to the conclusions arrived by our research group in our earlier work on the binary solutions of acetone with ethanol [24]. We had carried out FTIR spectroscopic studies and DFT calculations in that work and found that ethanol methyl/methylene stretching modes undergo shifts in the solutions even without the active participation of these groups in heterointeractions with acetone. The other interactions

happening in those solutions cause electron delocalization which affects the bond lengths of the ethanol methyl and methylene groups, therein producing shifts in their stretching modes. This reasoning may be applicable in the present work wherein the probable heterointeractions (*MXY ring/methyl*) $C-H\cdots O$ (*carbonyl oxygen of MA*) adjacent to the MA methyl group can be one among the factors behind the shifts in $\nu_{as}(CH_3)$ and $\nu_s(CH_3)$ modes of MA in MAMXY solution. No shift in ν $(C-C-O)$ mode of MA in the binary solution may not be a factor to rule out the possibilities for the interactions: (*MXY ring/methyl*) $C-H\cdots O$ (*alkoxy oxygen of MA*). Because the presence of these interactions along with the other heterointeractions and/or the probable dissociation of MA in the solution may affect the bond lengths of MA such that there is no shift in ν $(C-C-O)$ mode of MA. On the same lines, the no shift in the ring deformation mode of MXY in the solution (Fig. 1c, Table 1) may be a resultant of the interactions: (*MXY ring/methyl*) $C-H\cdots O$ (*carbonyl oxygen of MA*), (*MXY ring/methyl*) $C-H\cdots O$ (*alkoxy oxygen of MA*) and (*MA*)$C-H\cdots\pi$ (*MXY*).

3.2. DFT calculations

The possibility for the presence of higher order H-bonded molecular networks either in pure MA or in the MAMXY binary solution is limited because of the fact that non-classical H-bonds are usually very weak. Therefore, the DFT calculations are focused mainly on the MA dimers and 1:2 (MXY:MA) complexes. However, this does not mean that pure MA consists of only dimers and MXY always forms only the 1:2 complexes with MA. Higher order aggregates of MA molecules and MA-MXY complexes will be dealt with in a separate manuscript. In this present work, MA dimers of different geometries (Fig. 2), MXY monomer (Fig. 3a) and MA-MXY complexes (Figs. 3b, c, d and 4) of different geometries were optimized and theoretical unscaled wavenumbers (Tables S1 and S2 – the Supplementary files) of various vibrational modes in these structures have been calculated. Scaling of the theoretical wavenumbers has not been done in the present work. Because in the present work we are concerned only about the pattern of shifts in the theoretical wavenumbers in the complex molecules when compared to that in MA dimers, MXY monomer. Therefore, scaling of these numbers by multiplying with a common factor is not going to affect their shifts (red or blue). This point has already been mentioned by our research group in our earlier work [20]. The average of the wavenumbers corresponding to vibrational modes in all the MA dimers, MXY monomer and that of the modes in MA-MXY complexes have been compared in Table 2. From the comparison it is clear that the pattern of variation (red or blue shifts) of the vibrational modes (except the ν $(C-C-O)$ mode of MA and ring deformation mode of MXY) in the complex molecules relative to that the MA dimers, MXY monomer is in good agreement with the experimental data (Fig. 1, Table 1). The theoretical wavenumbers with respect to the ν $(C-C-O)$ mode of MA and ring deformation mode of MXY in the complex molecules have undergone shifts when compared to that in the MA dimers/MXY monomer. This result contradicts the experimental findings in which no shifts in these modes have been observed in the binary solution MAMXY. This kind of discrepancy has earlier been reported by our research group in recent times [20,23] in which we had observed contradictions with at least one vibrational mode. Moreover, in the present work the theoretical wavenumber corresponding to ring deformation

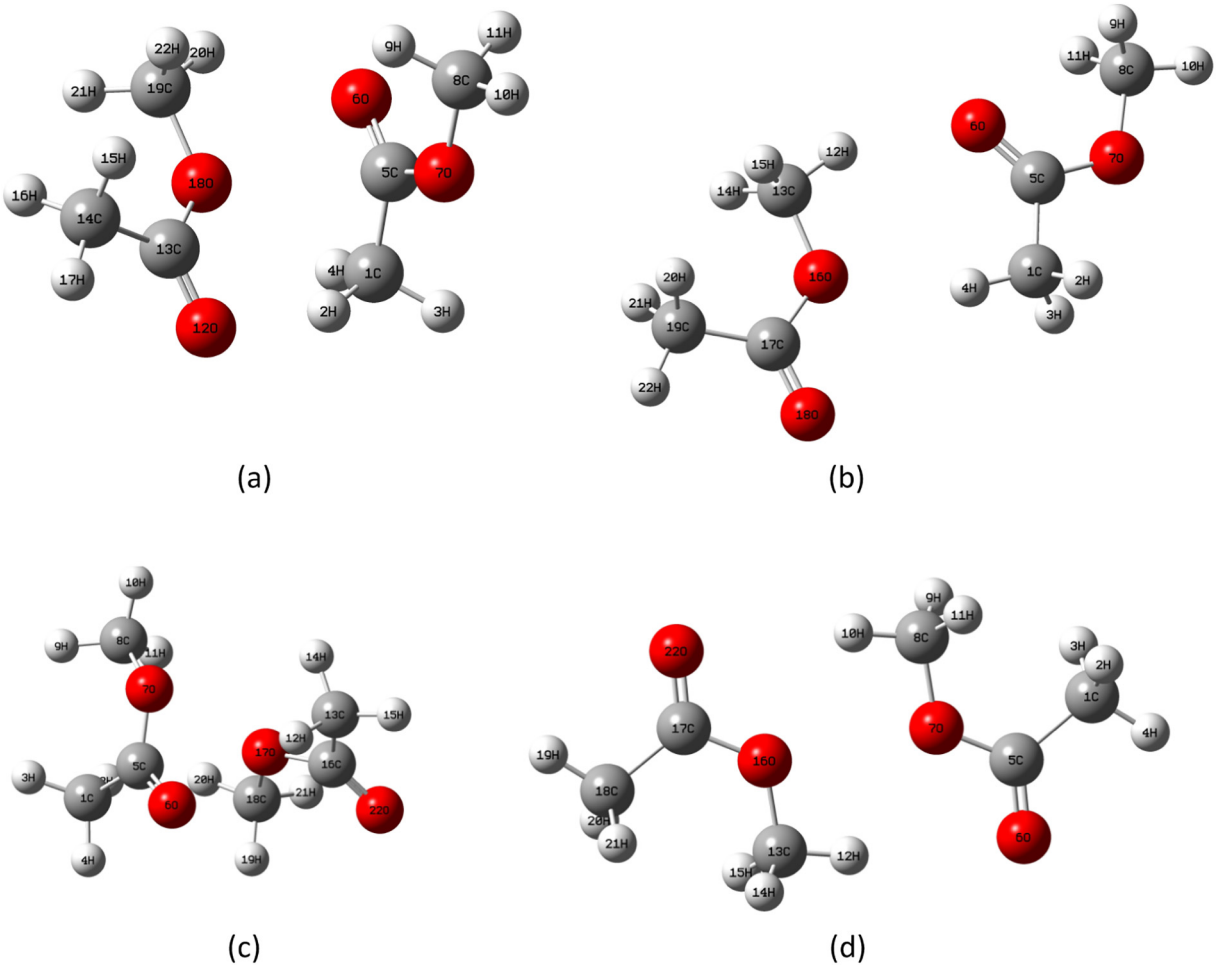

Fig. 2. Optimized geometry of (a) MA dimer1 (b) MA dimer2 (c) MA dimer3 (d) MA dimer4. The labels and symbols should be correlated with Table 3.

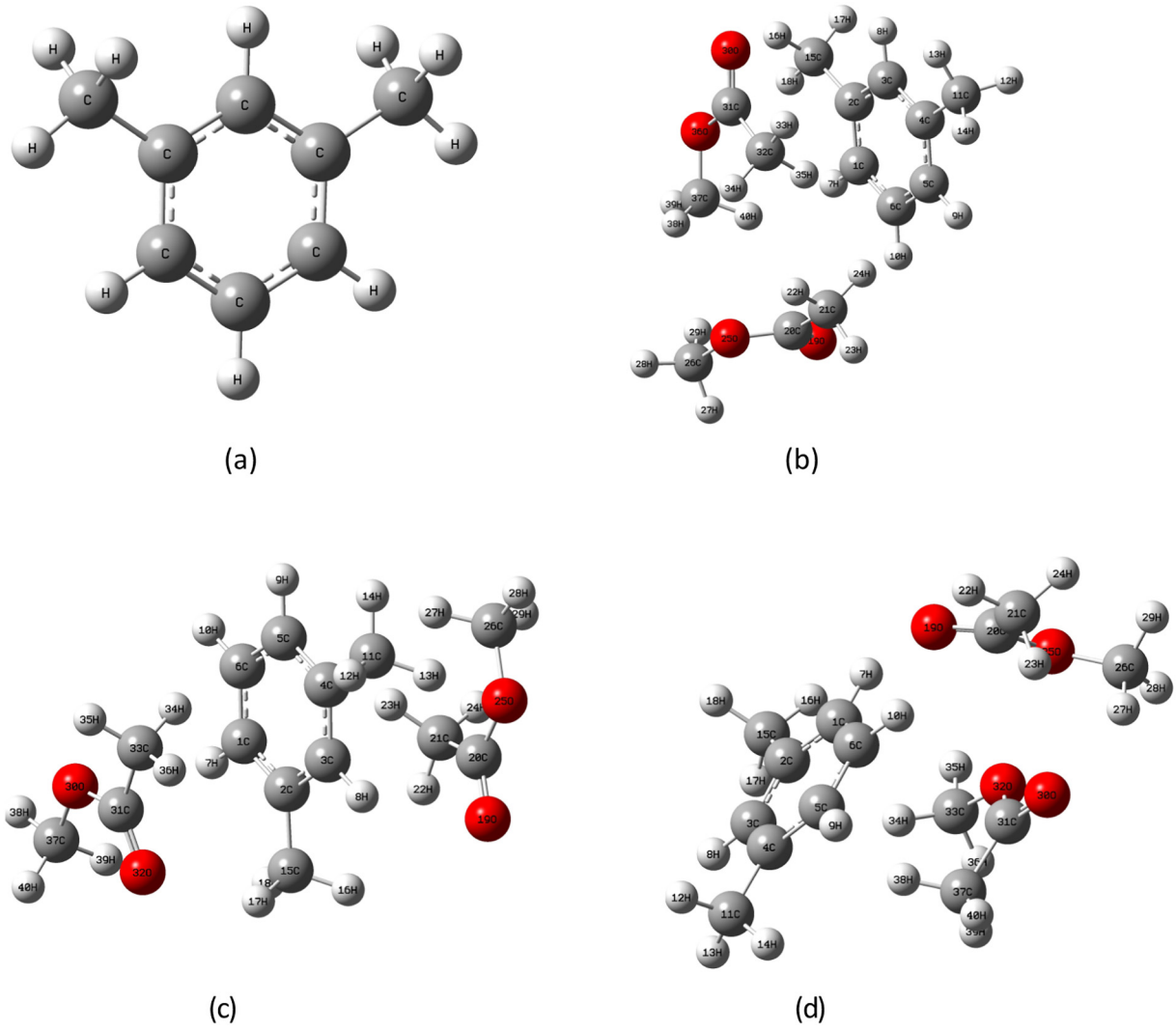

Fig. 3. Optimized geometry of (a) m-xylene (b) MAMXY - complex1 (c) MAMXY – complex2 (d) MAMXY – complex3. The labels and symbols should be correlated with Table 4.

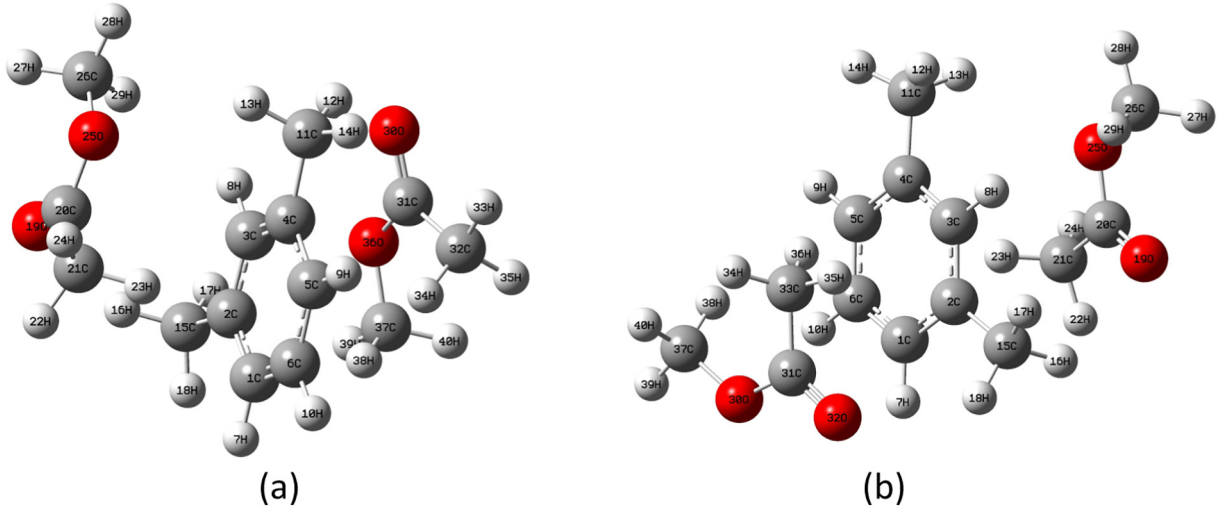

Fig. 4. Optimized geometry of (a) MAMXY – complex4 (b) MAMXY – complex5. The labels and symbols should be correlated with Table 5.

mode of MXY does not undergo any shift in the complex molecules if we round off those numbers to nearest value i.e., 1273 cm^{-1} in Table 2 for comparison. Therefore, it can be opined that the MA dimers and MA-MXY complexes investigated in the present work have more chances to exist. The theoretical vibrational spectra of the optimized structures have been presented in Figs. S1–S3 – the Supplementary files.

In both the MA dimer1 and dimer2 (Fig. 2a and b), only one $C = O$ oxygen ($O12$ in MA dimer1 and $O6$ in MA dimer2) involves in H-bond interaction (Table 3). The $C - H\cdots O = C$ interaction in MA dimer2 (E (2) values 140.79 and 59.08 kJ/mol) is more stronger than that in MA dimer1(E(2) values 34.27 and 25.77 kJ/mol). The alkoxy oxygen too involves in hydrogen bond interactions (between $H2$ and $O18$ in MA dimer1, between $H4$ and $O16$, $H12$ and $O7$ in MA dimer2) in both these dimers but they are feeble in nature, as ascertained from the E (2) values. Only the alkoxy oxygen $O7$ contributes to dimerization in MA dimer3 (Fig. 2c, Table 3) via the H-bonds and not any of the carbonyl oxygens. Although the lone pair electrons of all the oxygens participate in H-bond interactions in MA dimer4 (Fig. 2d, Table 3), the overall E (2) values are smaller than that of the other dimers. This dimer4 is the weakest among all the dimers as per both the E(2) and interaction energy values. The coexistence of both the interactions $C - H\cdots O = C$ and $C - H\cdots O - C$ in MA dimer4 in which the latter has more strength, has drastically reduced its stability. Even though the lone pair electrons in MA dimer3 involve in much weaker interactions (smaller E(2) values) than that in dimer2, the former is slightly more stable (interaction energy −52.72 kJ/mol) than the later (interaction energy −52.07 kJ/mol). This type of relationship between the E(2) and interaction energy values, that can also be noticed when the dimer1 is compared with dimer2, has been reported in the earlier work [24]. Since dimer1 is more stable than the other dimers studied, the MA molecules may remain in dimer1 configuration for most of the time in pure liquid state.

From the E(2) profile of the relatively more stable dimer1, it is clear that only one of the two carbonyl oxygens ($O12$ in Fig. 2a) is involved in H-bond. Therefore, the two carbonyl bonds in this dimer have different bond strengths which affects their IR absorption frequencies. This in turn leads to the doublet of $C = O$ stretching peaks in the FTIR spectrum of pure MA (Fig. 1a, Table 1). This doublet is observed not only in pure MA but also in the FTIR spectrum of the binary solution MAMXY (Fig. 1c, Table 1). Unlike in the case of the MA dimers investigated in the present work, both the $C = O$ bonds in the MA- MXY complexes (Figs. 3 and 4) participate in the H-bond interactions but with different interaction strengths.

The stability of the five complexes, which are more stable than the MA dimers, investigated in the present work is in the following order, as can be disseminated from their interaction energies (Tables 3–5): MAMXY – complex4 > MAMXY – complex2 > MAMXY – complex5 > MAMXY – complex1 > MAMXY – complex3. Homo as well as heteromolecular interactions are present in MAMXY complexes1 and 3 while the remaining complexes have only heterointeractions. The $(MA)C - H\cdots\pi\,(MXY)$ heterointeraction arising out of the delocalization of the π electron of MXY is the strongest ($\pi_{C5-C6} \rightarrow \sigma^*_{C32-H35}$ in complex1, $\pi_{C4-C5} \rightarrow \sigma^*_{C33-H34}$ in complex2, $\pi_{C5-C6} \rightarrow \sigma^*_{C21-H23}$ in complex4 and $\pi_{C4-C5} \rightarrow \sigma^*_{C21-H23}$ in complex5) among all the interactions that are operative in all the complexes (Figs. 3 and 4, Tables 4 and 5), except complex3 in which the homointeraction (MA) $C - H\cdots O = C\,(MA)$ between $H23$ and $O30$ is the strongest and it is an indication that MA molecules prefer to associate among themselves rather than interacting with MXY in this particular complex. But speaking in terms of stability, this complex remains intact only for a shorter duration when compared with other complexes in the binary solution MAMXY because of its highest interaction energy (Table 4). Therefore, the interactions identified in MAMXY - complex3 may have only little role to play in the vibrational modes of MA/MXY in the MAMXY solution and the larger contribution may be from the most stable MAMXY – complex4 in which not only the MA-MA hyper conjugative homo interactions but the interactions involving the ring $C - H$ hydrogen of MXY are also absent. The absence of these interactions in MAMXY complexes 2 and 5 which have more stability next to MAMXY – complex4 can also be ascertained from Tables 4 and 5. The MAMXY complexes 1 and 3 which have homo molecular interactions between MA molecules in addition to the heterointeractions are relatively less stable than the other three complexes studied. Of these two complexes which have homointeractions among MA molecules, the MAMXY complex3 in which the alkoxy oxygen of one MA molecule interacts with the methyl hydrogen of another MA molecule is a bit more stable (Table 4) than complex3 in which it is the carbonyl oxygen that participates in the homointeraction.

Table 2
Comparison of the theoretical wavenumbers (unscaled) corresponding to vibrational modes of methyl acetate dimers (average of the values in 4 different geometries), m-xylene and the molecular complexes containing MA, MXY (average of the values in MAMXY-complex1, MAMXY-complex2…MAMXY-complex5).

Vibrational mode	Wavenumber (cm^{-1})		
	Methyl acetate dimers	m-Xylene	Molecular complexes
$\nu_{as}(CH_3)$	3150.99		3134.83
$\nu_s(CH_3)$	3038.89		3042.73
$\nu_{higher}\,(C = O)$	1805.35		1803.85
$\nu_{lower}\,(C = O)$	1788.88		1788.09
$\nu\,(C - C - O)$	1262.61		1261.38
$\nu_s(C - H)$		3178.83	3186.58
$\nu_{as}(C - H)$		3150.04	3159.11
$\nu_{as}(CH_3)$		3098.38	3088.30
Ring deformation		1272.78	1273.32

4. Conclusions

Based on our present investigation on the equimolar binary solution of MA with MXY the following conclusions can be arrived:

Table 3
Second order perturbation energy E(2) profile and interaction energy (both energies in kJ/mol) for MA dimers (Fig. 2).

MA dimer1 – Fig. 2a		MA dimer2 – Fig. 2b		MA dimer3 – Fig. 2c		MA dimer4 – Fig. 2d	
Interaction type	E(2)	Interaction type	E(2)	Interaction type	E(2)	Interaction type	E(2)
$\sigma_{C1-H2} \rightarrow \sigma^*_{O12-C13}$	1.46	$\sigma_{C1-H4} \rightarrow \sigma^*_{C13-O16}$	0.33	$n_{LP\,(1)O7} \rightarrow \sigma^*_{H12-C13}$	1.59	$n_{LP\,(2)O6} \rightarrow \sigma^*_{H12-C13}$	0.46
$\sigma_{O12-C13} \rightarrow \sigma^*_{C1-H2}$	0.92	$\sigma_{C5-O6} \rightarrow \sigma^*_{H12-C13}$	3.14	$n_{LP\,(2)O7} \rightarrow \sigma^*_{H12-C13}$	13.05	$n_{LP\,(1)O7} \rightarrow \sigma^*_{H12-C13}$	1.72
$n_{LP(1)\,O12} \rightarrow \sigma^*_{C1-H2}$	34.27	$\sigma_{C5-O7} \rightarrow \sigma^*_{H12-C13}$	0.88	$\sigma^*_{C5-O7} \rightarrow \sigma^*_{H12-C13}$	0.50	$n_{LP\,(1)O7} \rightarrow \sigma^*_{C13-H14}$	0.38
$n_{LP(2)\,O12} \rightarrow \sigma^*_{C1-H2}$	25.77	$n_{LP\,(1)O6} \rightarrow \sigma^*_{H12-C13}$	59.08	$\sigma_{H12-C13} \rightarrow \sigma^*_{O7-C8}$	0.20	$\sigma^*_{C5-O7} \rightarrow \sigma^*_{C13-H14}$	0.38
$\sigma^*_{C13-O18} \rightarrow \sigma^*_{C1-H2}$	0.20	$n_{LP\,(1)O6} \rightarrow \sigma^*_{C13-H14}$	0.79			$n_{LP\,(1)O16} \rightarrow \sigma^*_{C8-H9}$	0.20
		$n_{LP\,(2)O6} \rightarrow \sigma^*_{H12-C13}$	140.79			$n_{LP\,(1)O16} \rightarrow \sigma^*_{C8-H10}$	1.88
		$n_{LP\,(2)O6} \rightarrow \sigma^*_{C13-H15}$	0.42			$n_{LP\,(2)O22} \rightarrow \sigma^*_{C8-H10}$	0.58
		$\sigma_{H12-C13} \rightarrow \sigma^*_{C5-O6}$	3.22				
		$\sigma_{H12-C13} \rightarrow \pi^*_{C5-O6}$	0.25				
		$\sigma_{C13-H14} \rightarrow \sigma^*_{C5-O6}$	0.29				
Interaction energy	−55.09		−52.07		−52.72		−24.13

Table 4
Second order perturbation energy E(2) profile and interaction energy (both energies in kJ/mol) for molecular complexes containing MA and MXY.

MAMXY - complex1 – Fig. 3b		MAMXY - complex2 – Fig. 3c		MAMXY - complex3 – Fig. 3d	
Interaction type	E(2)	Interaction type	E(2)	Interaction type	E(2)
$\pi_{C5-C6} \rightarrow \sigma^*_{C21-H24}$	2.22	$\pi_{C1-C6} \rightarrow \sigma^*_{C21-H23}$	1.59	$\sigma_{C15-H16} \rightarrow \pi^*_{O19-C20}$	0.25
$\pi^*_{C5-C6} \rightarrow \sigma^*_{C21-H24}$	0.42	$\pi_{C2-C3} \rightarrow \sigma^*_{C21-H24}$	0.38	$\pi_{C1-C2} \rightarrow \sigma^*_{C33-H34}$	1.00
$\pi_{C1-C2} \rightarrow \sigma^*_{C32-H35}$	0.25	$\pi_{C4-C5} \rightarrow \sigma^*_{C26-H27}$	2.13	$\pi_{C1-C2} \rightarrow \sigma^*_{C37-H38}$	0.29
$\pi_{C1-C2} \rightarrow \sigma^*_{C37-H40}$	0.96	$\pi_{C1-C6} \rightarrow \sigma^*_{C33-H34}$	0.42	$\pi_{C3-C4} \rightarrow \sigma^*_{C37-H38}$	2.05
$\pi_{C3-C4} \rightarrow \sigma^*_{C32-H34}$	0.50	$\pi_{C2-C3} \rightarrow \sigma^*_{C33-H35}$	0.25	$\pi_{C5-C6} \rightarrow \sigma^*_{C37-H39}$	0.58
$\pi_{C5-C6} \rightarrow \sigma^*_{C32-H35}$	2.38	$\pi_{C4-C5} \rightarrow \sigma^*_{C33-H34}$	2.22	$\pi^*_{C1-C2} \rightarrow \sigma^*_{C33-H34}$	0.54
$\pi^*_{C1-C2} \rightarrow \sigma^*_{C37-H40}$	0.84	$\sigma_{C15-H17} \rightarrow \pi^*_{C31-O32}$	0.67	$\pi_{O19-C20} \rightarrow \sigma^*_{C1-H7}$	0.58
$n_{LP\,(1)O19} \rightarrow \sigma^*_{C6-H10}$	0.54	$\pi_{O19-C20} \rightarrow \sigma^*_{C15-H16}$	0.33	$\pi_{O19-C20} \rightarrow \sigma^*_{C15-H16}$	0.63
$n_{LP\,(2)O19} \rightarrow \sigma^*_{C6-H10}$	0.63	$n_{LP\,(1)O19} \rightarrow \sigma^*_{C15-H16}$	0.21	$n_{LP\,(1)O19} \rightarrow \sigma^*_{C1-H7}$	0.79
$\pi_{O19-C20} \rightarrow \sigma^*_{C37-H40}$	0.54	$n_{LP\,(2)O19} \rightarrow \sigma^*_{C15-H16}$	0.46	$n_{LP\,(1)O19} \rightarrow \sigma^*_{C15-H16}$	1.84
$\sigma_{C26-H29} \rightarrow \sigma^*_{O36-C37}$	0.84	$n_{LP\,(1)O25} \rightarrow \sigma^*_{C11-H13}$	0.54	$n_{LP\,(2)O19} \rightarrow \sigma^*_{C1-H7}$	2.43
$n_{LP\,(2)O25} \rightarrow \sigma^*_{C37-H38}$	0.38	$n_{LP\,(2)O25} \rightarrow \sigma^*_{C11-H13}$	0.84	$\pi^*_{O19-C20} \rightarrow \sigma^*_{C15-H16}$	0.21
$\pi_{O30-C31} \rightarrow \sigma^*_{C15-H16}$	1.00	$\sigma^*_{C20-O25} \rightarrow \sigma^*_{C11-H13}$	0.25	$\pi_{O19-C20} \rightarrow \sigma^*_{C33-H36}$	0.29
$\sigma_{C37-H40} \rightarrow \pi^*_{C1-C2}$	0.88	$\pi_{C31-O32} \rightarrow \sigma^*_{C15-H16}$	0.21	$n_{LP\,(2)O19} \rightarrow \sigma^*_{C33-H35}$	0.38
$n_{LP\,(1)O30} \rightarrow \sigma^*_{C15-H16}$	0.21	$\pi_{C31-O32} \rightarrow \sigma^*_{C15-H17}$	1.26	$n_{LP\,(2)O25} \rightarrow \sigma^*_{C33-H35}$	0.29
$n_{LP\,(2)O30} \rightarrow \sigma^*_{C15-H16}$	0.88	$n_{LP\,(1)O32} \rightarrow \sigma^*_{C15-H17}$	1.13	$\sigma_{C33-H34} \rightarrow \pi^*_{C1-C2}$	0.46
$n_{LP\,(2)O36} \rightarrow \sigma^*_{C15-H17}$	0.38	$\pi^*_{C31-O32} \rightarrow \sigma^*_{C15-H17}$	0.25	$\pi_{O30-C31} \rightarrow \sigma^*_{C21-H23}$	0.92
				$n_{LP\,(1)O30} \rightarrow \sigma^*_{C21-H23}$	0.96
				$n_{LP\,(2)O30} \rightarrow \sigma^*_{C21-H23}$	4.06
				$n_{LP\,(2)O30} \rightarrow \sigma^*_{C26-H27}$	0.46
				$n_{LP\,(1)O32} \rightarrow \sigma^*_{C26-H27}$	0.54
				$n_{LP\,(1)O32} \rightarrow \sigma^*_{C26-H29}$	0.42
				$\sigma^*_{C31-O32} \rightarrow \sigma^*_{C26-H29}$	0.29
Interaction energy	−79.02		−84.30		−73.09

Table 5
Second order perturbation energy E(2) profile and interaction energy (both energies in kJ/mol) for molecular complexes MAMXY - complex4 and MAMXY - complex5.

MAMXY - complex4 – Fig. 4a		MAMXY - complex5 – Fig. 4b	
Interaction type	E(2)	Interaction type	E(2)
$\pi_{C3-C4} \rightarrow \sigma^*_{C21-H23}$	0.38	$\pi_{C1-C6} \rightarrow \sigma^*_{C21-H23}$	0.96
$\pi_{C5-C6} \rightarrow \sigma^*_{C21-H23}$	1.92	$\pi_{C4-C5} \rightarrow \sigma^*_{C21-H23}$	1.26
$\sigma_{C15-H16} \rightarrow \pi^*_{O19-C20}$	0.46	$\sigma_{C15-H16} \rightarrow \pi^*_{O19-C20}$	0.25
$\pi_{C1-C2} \rightarrow \sigma^*_{C37-H38}$	1.88	$\pi_{C1-C6} \rightarrow \sigma^*_{C33-H36}$	0.29
$\pi_{C3-C4} \rightarrow \sigma^*_{C32-H35}$	0.38	$\pi_{C1-C6} \rightarrow \sigma^*_{C37-H38}$	0.58
$\pi_{C5-C6} \rightarrow \sigma^*_{C32-H34}$	1.26	$\pi_{C2-C3} \rightarrow \sigma^*_{C33-H34}$	0.46
$\sigma_{C11-H12} \rightarrow \pi^*_{O30-C31}$	0.25	$\pi_{C4-C5} \rightarrow \sigma^*_{C33-H36}$	1.09
$\pi_{O19-C20} \rightarrow \sigma^*_{C15-H16}$	1.26	$\sigma_{C15-H18} \rightarrow \pi^*_{C31-O32}$	0.38
$n_{LP\,(1)O19} \rightarrow \sigma^*_{C15-H16}$	1.13	$\pi^*_{C1-C6} \rightarrow \sigma^*_{C37-H38}$	0.54
$n_{LP\,(2)O19} \rightarrow \sigma^*_{C15-H16}$	0.29	$\pi_{O19-C20} \rightarrow \sigma^*_{C15-H16}$	0.29
$n_{LP\,(1)O25} \rightarrow \sigma^*_{C11-H13}$	0.63	$n_{LP\,(1)O19} \rightarrow \sigma^*_{C15-H16}$	0.25
$n_{LP\,(2)O25} \rightarrow \sigma^*_{C11-H13}$	0.58	$n_{LP\,(2)O19} \rightarrow \sigma^*_{C15-H16}$	0.42
$\pi^*_{O19-C20} \rightarrow \sigma^*_{C15-H16}$	0.25	$n_{LP\,(1)O25} \rightarrow \sigma^*_{C11-H13}$	0.50
$\sigma^*_{C20-O25} \rightarrow \sigma^*_{C11-H13}$	0.38	$n_{LP\,(2)O25} \rightarrow \sigma^*_{C11-H13}$	0.46
$\pi_{O30-C31} \rightarrow \sigma^*_{C11-H12}$	0.84	$\sigma^*_{C20-O25} \rightarrow \sigma^*_{C11-H13}$	0.33
$\sigma_{C37-H38} \rightarrow \pi^*_{C1-C2}$	0.25	$\pi_{C31-O32} \rightarrow \sigma^*_{C15-H18}$	0.71
$n_{LP\,(1)O30} \rightarrow \sigma^*_{C11-H12}$	0.71	$\sigma_{C37-H38} \rightarrow \pi^*_{C1-C6}$	0.79
$n_{LP\,(2)O30} \rightarrow \sigma^*_{C11-H12}$	0.84	$n_{LP\,(1)O32} \rightarrow \sigma^*_{C15-H18}$	0.63
$n_{LP\,(1)O36} \rightarrow \sigma^*_{C15-H17}$	0.21		
$n_{LP\,(2)O36} \rightarrow \sigma^*_{C15-H17}$	0.46		
Interaction energy	−89.96		−83.58

- In pure liquid state, MA molecules can form dimers of four different configurations. Both the interactions $C - H\cdots O = C$ and $C - H\cdots O - C$ can coexist in three of the above mentioned four dimers. The left alone dimer (MA dimer3) in which there is $C - H\cdots O - C$ interaction alone is less stable than the MA dimer1 in which the interactions $C - H\cdots O = C$ are stronger than the interactions $C - H\cdots O - C$. If the interactions $C - H\cdots O - C$ dominate over the interactions $C - H\cdots O = C$, as in case of MA dimer4 the stability becomes the least.
- The most stable dimer is the MA dimer1 followed by MA dimer3, succeeded by MA dimer2.
- All these dimers are highly unstable in comparison to the five 1:2 (MXY: MA) complexes investigated in the present work. Therefore, the dimers dissociate in the solution MAMXY and these complex molecules are formed. In all the complexes except the MAMXY - complex3, the heterointeractions $(MA)C - H\cdots\pi$ (MXY) are more stronger than any other interactions. In MAMXY - complex3, the homointeraction $(MA)C - H\cdots O = C$ (MA) among the two MA molecules is the strongest. This scenario drastically affects its stability which is the least among all the complex molecules. Another homointeraction $(MA)C - H\cdots O - C$ (MA) is also identified in this complex.
- When there are no homointeractions among MA molecules in the complexes (MAMXY - complex4, MAMXY – complex2 and MAMXY - complex5) the stability of the complexes is more. In these complexes only the methyl hydrogen of MXY involves in heteromolecular H-bonds and not the hydrogen atom attached to the ring carbon. When the latter hydrogen is involved in H-bonds with MA in the other two complexes their stability is reduced. Overall, the MAMXY - complex4 is the most stable among all the complexes.

Supplementary data to this article can be found online at https://doi.org/10.1016/j.molliq.2020.113491.

CRediT authorship contribution statement

N.K. Karthick: Writing - original draft, Investigation. **G. Arivazhagan:** Conceptualization, Writing - review & editing, Supervision. **P.P. Kannan:** Validation, Formal analysis, Writing - review & editing.

Declaration of competing interest

The authors declare the following personal relationships which may be considered as potential competing interests: Dr. G. Parthipan (personal reason) and Dr. V. Ramakrishnan (personal reason).

Acknowledgement

The financial support to the present work from the Department of Science and Technology, New Delhi, India through SERB Fast Track Young Scientist Research Project (SR/FTP/PS-011/2012) is gratefully

acknowledged by one of the authors GA. Another author NKK is thankful to DST, New Delhi, India for the award of Project Fellowship through this project.

References

[1] G.C. Pimentel, A.L. McClellan, The Hydrogen Bond, W. H. Freeman & Co, San Francisco, 1960.
[2] D. Braga, F. Grepioni, Acc. Chem. Res. 33 (2000) 601–608.
[3] G. Pescitelli, L. Bari, N. Berova, Chem. Soc. Rev. 43 (2014) 5211–5233.
[4] G. Stogiannidis, S. Tsigoias, P. Mpourazanis, S. Boghosian, S. Kaziannis, A.G. Kalampounias, Chem. Phys. 522 (2019) 1–9.
[5] S.D. Fried, S. Bagchi, S.G. Boxer, J. Am. Chem. Soc. 135 (2013) 11181–11192.
[6] A. Barth, C. Zscherp, Q. Rev. Biophys. 35 (2002) 369–430.
[7] F.X. Sunahori, N. Borho, X. Liu, Y. Xu, J. Chem. Phys. 135 (2011), 234310. .
[8] I.M. Pazos, A. Ghosh, M.J. Tucker, F. Gai, Angew. Chem. Int. Ed. 53 (2014) 6080–6084.
[9] M. Banno, K. Ohta, K. Tominaga, J. Raman Spectrosc. 39 (2008) 1531–1537.
[10] M. Candelaresi, M. Pagliai, M. Lima, R. Righini, J. Phys. Chem. A 113 (2009) 12783–12790.
[11] B. Fang, T. Wang, X. Chen, T. Jin, R. Zhang, W. Zhuang, J. Phys. Chem. B 119 (2015) 12390–12396.
[12] J.A. Frey, S. Leutwyler, J. Phys. Chem. A 110 (2006) 12512–12518.
[13] R. Vargas, J. Garza, R.A. Friesner, H. Stern, B.P. Hay, D.A. Dixon, J. Phys. Chem. A 105 (2001) 4963–4968.
[14] N.V. Sastry, R.R. Thakor, M.C. Patel, J. Mol. Liq. 144 (2009) 13–22.
[15] P.P. Kannan, G. Arivazhagan, T. Sangeetha, N.K. Karthick, A.C. Kumbharkhane, Spectrochim. Acta A 222 (2019), 117162. .
[16] P.P. Kannan, N.K. Karthick, G. Arivazhagan, Spectrochim. Acta A 229 (2020), 117892. .
[17] M.J. Frisch, G.W. Trucks, H.B. Schlegel, G.E. Scuseria, M.A. Robb, J.R. Cheeseman, G. Scalmani, V. Barone, B. Mennucci, G.A. Petersson, H. Nakatsuji, M. Caricato, X. Li, H.P. Hratchian, A.F. Izmaylov, J. Bloino, G. Zheng, J.L. Sonnenberg, M. Hada, M. Ehara, K. Toyota, R. Fukuda, J. Hasegawa, M. Ishida, T. Nakajima, Y. Honda, O. Kitao, H. Nakai, T. Vreven, J.A. Montgomery Jr., J.E. Peralta, F. Ogliaro, M. Bearpark, J.J. Heyd, E. Brothers, K.N. Kudin, V.N. Staroverov, T. Keith, R. Kobayashi, J. Normand, K. Raghavachari, A. Rendell, J.C. Burant, S.S. Iyengar, J. Tomasi, M. Cossi, N. Rega, J.M. Millam, M. Klene, J.E. Knox, J.B. Cross, V. Bakken, C. Adamo, J. Jaramillo, R. Gomperts, R.E. Stratmann, O. Yazyev, A.J. Austin, R. Cammi, C. Pomelli, J.W. Ochterski, R.L. Martin, K. Morokuma, V.G. Zakrzewski, G.A. Voth, P. Salvador, J.J. Dannenberg, S. Dapprich, A.D. Daniels, O. Farkas, J.B. Foresman, J.V. Ortiz, J. Cioslowski, D.J. Fox, Gaussian 09, Revision D.01, Gaussian, Inc, Wallingford CT, 2010.
[18] A.D. Becke, C. Lee, W. Yang, R.G. Parr, J. Chem. Phys. 98 (1993) 5648–5652Phys. Rev. B 37 (1993) 785–789.
[19] S. Grimme, J. Antony, S. Ehrlich, H. Krieg, J. Chem. Phys. 132 (2010), 154104. .
[20] N.K. Karthick, G. Arivazhagan, P.P. Kannan, A. Mahendraprabu, A.C. Kumbharkhane, S.S. Shaikh, Y.S. Joshi, J. Mol. Liq. 251 (2018) 385–393.
[21] R. Knaanie, J. Sebek, M. Tsuge, N. Myllys, L. Khriachtchev, M. Rasanen, B. Albee, E.O. Potma, R.B. Gerber, J. Phys. Chem. A 120 (19) (2016) 3380–3389.
[22] N.K. Karthick, G. Arivazhagan, R. Shanmugam, J. Mol. Struct. 1173 (2018) 456–461.
[23] N.K. Karthick, G. Arivazhagan, P.P. Kannan, A.C. Kumbharkhane, Y.S. Joshi, J. Mol. Struct. 1192 (2019) 208–216.
[24] D.L. Jadhav, N.K. Karthick, P.P. Kannan, R. Shanmugam, A. Elangovan, G. Arivazhagan, J. Mol. Struct. 1130 (2017) 497–502.